第39卷第6期
2023年6月

无 机 化 学 学 报
CHINESE JOURNAL OF INORGANIC CHEMISTRY

Vol.39 No.6
1122-1130

吡咯腙对溶酶体中Hg^{2+}的荧光成像

王 震[1] 李思媛[2] 王 元[1] 吴伟娜[1] 张 磊*,[1] 陈 忠*,[2] 闫玲玲[3]

([1]河南理工大学化学化工学院,焦作 454000)

([2]江西科技师范大学材料与机电学院,南昌 330013)

([3]河南理工大学物理与电子信息学院,焦作 454000)

摘要: 合成了一种新的吡咯腙探针**1**,用于Hg^{2+}的比色和荧光开启检测。探针**1**对Hg^{2+}的检测限为45 nmol·L^{-1},缔合常数为5.78×10^8 L·mol^{-1}。值得注意的是,工作pH范围为4.0~10.0。Job曲线和MS数据证实探针与Hg^{2+}形成1∶1的配合物。通过^{1}H NMR、时间分辨荧光光谱和密度泛函理论(DFT)计算系统研究了探针与Hg^{2+}的配位模式。此外,由于吗啉基团的存在,探针可以检测HeLa细胞溶酶体中的Hg^{2+}。

关键词: 细胞成像;荧光探针;Hg^{2+};腙;溶酶体;吡咯

中图分类号: O614.24+3 **文献标识码:** A **文章编号:** 1001-4861(2023)06-1122-09

DOI: 10.11862/CJIC.2023.083

Pyrrole-based hydrazone for fluorescent imaging of Hg^{2+} in lysosomes

WANG Zhen[1] LI Si-Yuan[2] WANG Yuan[1] WU Wei-Na[1]

ZHANG Lei*,[1] CHEN Zhong*,[2] YAN Ling-Ling[3]

([1]*College of Chemistry and Chemical Engineering, Henan Polytechnic University, Jiaozuo, Henan* 454000 *China*)

([2]*School of Materials and Mechanical and Electrical Engineering, Jiangxi Science and Technology Normal University, Nanchang* 330013 *China*)

([3]*School of Physics and Electronic Information Engineering, Henan Polytechnic University, Jiaozuo, Henan* 454000 *China*)

Abstract: A novel pyrrole-based hydrazone has been synthesized for colorimetric and fluorescent turn-on detection of Hg^{2+} ions. A 1∶1 binding ratio of the Hg^{2+} complex has been obtained from Job′s plots and MS data. The coordination mode was systematically investigated by ^{1}H NMR, time-resolved fluorescence spectroscopy, and density functional theory (DFT) calculations. The limit of detection of **1** for Hg^{2+} was as low as 45 nmol·L^{-1} with an association constant of 5.78×10^8 L·mol^{-1}. It is worth noting that the response of **1** to Hg^{2+} was good in a pH range of 4.0 to 10.0. In addition, owing to the existence of the morpholine group, the probe can detect lysosomal Hg^{2+} in HeLa cells.

Keywords: cell imaging; fluorescent probe; Hg^{2+}; hydrazone; lysosome; pyrrole

Fluorescent probes can be used as an efficient tool for the detection and imaging of biological trace species, pesticide residues and heavy metal cations[1]. Among various heavy metal cations, Hg^{2+} is extremely toxic, and it becomes methylmercury which accumulates in the body through the food chain, leading to a series of mental illnesses and the well-known Minamata disease[2-4]. Consequently, selective and sensitive flu-

收稿日期:2022-04-03。收修改稿日期:2023-04-27。

国家自然科学基金(No.21907023,21001040,61964008)、河南省重点研发与推广专项科技攻关项目(No.232102320092)、江西省自然科学基金(No.20212BAB204017)、河南省高校基本科研业务费项目(No.NSFRF230402)、河南理工大学“双一流”创建工程项目(No.AQ20230745,AQ20230754)和河南理工大学研究生教改项目(No.2021YJ16)资助。

*通信联系人。E-mail:leizh2008@163.com,chenzhonglzu@hotmail.com

orescent probes for Hg^{2+} detection are highly desirable.

Generally, most of papers published about Hg^{2+} probes have investigated the high thiophilicity of Hg^{2+}[5-8]. Furthermore, rhodamine[6-7,9,12], coumarin[10], and naphthalimide[7] have been frequently employed as signal fluorophores for the probe design. Some of them have been utilized for fluorescence imaging of Hg^{2+} in living cells (Table S1, Supporting information)[5-14]. It is worth noting that lysosomes digest unwanted substances and cell fragments and contain a variety of hydrolases, so they are considered "enzyme banks" or "cell cleaners" in cells[15]. In fact, Hg^{2+} has been found to accumulate in lysosomes, causing abnormal lysosomal pH fluctuation, which is closely associated with lysosome dysfunctions[16]. In this regard, lysosomes are one of the important organelle targets for Hg^{2+} toxicity[17]. However, the probes that can be used in lysosomes for Hg^{2+} detection are barely reported[5-6,11]. It is well known that the pH of lysosomes in normal cells ranges from 4.5 to 6.0, while that of cancer cells is even lower[18]. Nevertheless, some of the reported probes, especially those based on rhodamine backbone, could not perform normally under such extremely acidic conditions[12]. In this regard, it is still a great challenge to the development of lysosome-targeting probes toward Hg^{2+}.

Recently, our group reported a pyrrole-containing bis-hydrazone (**1a**, Scheme 1) capable of detecting Hg^{2+} in real water samples[14]. Herein, a lysosome-targeting group of 4-(2-aminoethyl)morpholine was introduced to **1a** to fabricate a simple and effective fluorescent turn-on probe **1** for Hg^{2+} detection in lysosomes of HeLa cells. It is worth noting that the primary starting material, 5-formyl-2,4-dimethyl-1*H*-pyrrole-3-carboxylic acid, is a commercial intermediate of Sunitinib (an inhibitor used in cancer therapies) favoring the real-world application of the as-synthesized probe.

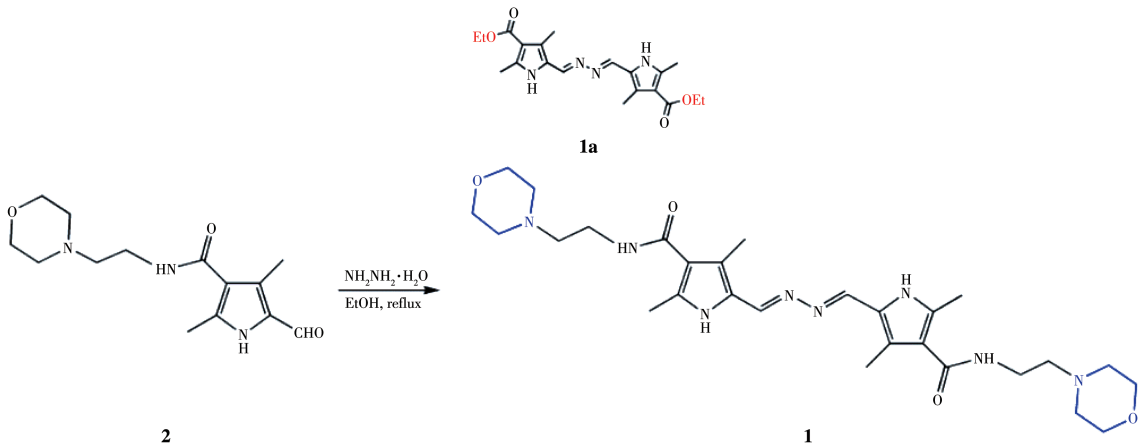

Scheme 1　Synthesis route of probe **1**

1　Experimental

1.1　Materials and instrumentation

Solvents and starting materials for syntheses were purchased commercially and used as received. Elemental analyses were carried out on an Elemental Vario EL analyzer. ^{1}H NMR spectra were recorded on a Bruker AV400 NMR spectrometer in DMSO-d_6 solution. The UV spectra were recorded on a Purkinje General TU-1800 spectrophotometer. Fluorescence spectra were determined on a Varian CARY Eclipse spectrophotometer, in the measurements of emission and excitation spectra the pass width was 5 nm. Time-resolved photoluminescence spectra were determined on an Edinburgh FLS980 spectrophotometer. ESI-MS spectra were obtained on a Bruker Daltonics Esquire 6000 mass spectrometer. The cytotoxic effect exerted by 1 on cultured HeLa cells was ascertained by a standard MTT assay according to the literature method[19]. Fluorescent images were taken on Zeiss Leica inverted epi-fluorescence/reflectance laser scanning confocal microscope.

1.2　Synthesis of 1

5-Formyl-2,4-dimethyl-1*H*-pyrrole-3-carboxylic

acid (2-morpholin-4-yl-ethyl)-amide (**2**) was prepared from 5-formyl-2,4-dimethyl-1*H*-pyrrole-3-carboxylic acid according to literature method[20]. Hydrazinium hydroxide (100 mg, 85%, 1.7 mmol) and **2** (279 mg, 1 mmol) were added to an EtOH solution (10 mL). The mixture was refluxed for 3 h with two drops of acetic acid. After cooling to room temperature, the separated solid was filtered, washed with EtOH, and then dried in air. Yield: 58%. Anal. Calcd. for $C_{28}H_{42}N_8O_4$(%): C, 60.63; H, 7.63; N, 20.20. Found(%): C, 60.48; H, 7.78; N, 20.33. ^{1}H NMR (400 MHz, DMSO-d_6): δ 11.35 (s, 1H, NH), 8.40 (s, 1H, CH), 7.24 (s, 1H, NH), 3.57 (t, 4H, 2CH_2), 3.30 (2H, merged by peak of H_2O), 2.41-2.44 (m, 8H, 4CH_2), 2.35 (s, 3H, CH_3), 2.25 (s, 3H, CH_3). ^{13}C NMR was not recorded due to the poor solubility of **1**. ESI-MS: *m/z*=555.321 8 for $[M+H]^+$ (Calcd. 555.330 0), 278.179 8 for $[M+2H]^{2+}$ (Calcd. 278.175 0), 185.787 0 for $[M+3H]^{3+}$ (Calcd. 185.786 6).

1.3 General UV-Vis and fluorescence spectra measurements

The spectral analyses were accomplished in EtOH/H_2O (7∶3, *V*/*V*) solution at room temperature. The concentration of probe **1** for UV-Vis and fluorescence measurement was 10 μmol·L^{-1}. Solutions of metal ions were prepared with nitrate or chloride salts in H_2O. UV-Vis and fluorescence spectrophotometric titration were conducted directly in a 2 mL cuvette by successive addition of corresponding chemical reagent using a microliter syringe. Upon addition of every aliquot, the solution was well mixed then the spectrum was measured.

2 Results and discussion

2.1 Synthesis and characterization

Probe **1** was produced by the condensation of **2** and hydrazinium hydroxide in a moderate yield, and was further characterized by elemental analyses, ^{1}H NMR, and ESI-MS methods. It should be noted that the peak of one CH_2 group was covered by the H_2O peak in the ^{1}H NMR spectrum of **1** (Fig.S1), which is assumed according to the spectrum of **2** shown in Fig.S2.

2.2 UV-Vis spectroscopic studies for Hg^{2+} sensor activity

The absorption spectrum of probe **1** (10 μmol·L^{-1}) in EtOH/H_2O (7∶3, *V*/*V*) solution displayed one band centered at 380 nm (Fig. 1a), attributed to the n-π* transition of imine units[14]. When probe **1** bound to Hg^{2+} (3 equiv.), the band had an obvious redshift to 413 nm, a hyperchromatic effect, along with the generation of a shoulder at 440 nm, assigned to the ligand to metal charge transfer (LMCT)[13]. This finding indicates that

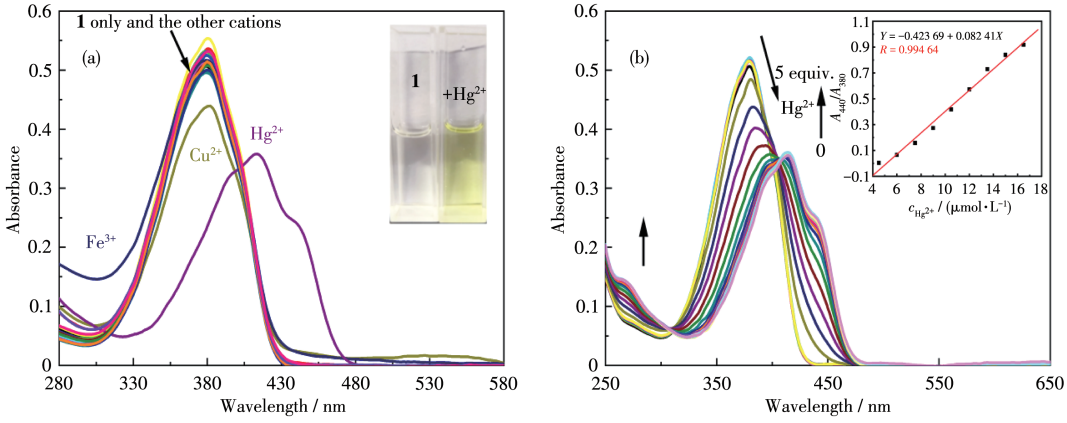

Inset in a: the color change of **1** solution in the presence of Hg^{2+}; Inset in b: the absorbance ratio of A_{440}/A_{380} as a function of Hg^{2+} concentration (4.5-16.5 μmol·L^{-1})

Fig.1 (a) UV-Vis spectra of 10 μmol·L^{-1} probe **1** in EtOH/H_2O (7∶3, *V*/*V*) solution with 3 equiv. of metal ions: Ag^+, Al^{3+}, Ca^{2+}, Cd^{2+}, Co^{2+}, Cr^{3+}, Cu^{2+}, Fe^{3+}, Hg^{2+}, K^+, Mg^{2+}, Mn^{2+}, Na^+, Ni^{2+}, Pb^{2+}, and Zn^{2+} ions and blank; (b) UV-Vis spectra of 10 μmol·L^{-1} probe **1** upon the addition of Hg^{2+} (0-5 equiv.) in EtOH/H_2O (7∶3, *V*/*V*) solution

the N atom of the imine bond is involved in the coordination with Hg^{2+}. The change of the color of the liquid in the cuvette from colorless to yellow leads to the conclusion that the response of probe **1** to Hg^{2+} is more pronounced and more selective than the other metal ions (3 equiv.) tested (Fig. 1a, Inset), including Ag^+, Al^{3+}, Ca^{2+}, Cd^{2+}, Co^{2+}, Cr^{3+}, Cu^{2+}, Fe^{3+}, K^+, Mg^{2+}, Mn^{2+}, Na^+, Ni^{2+}, Pb^{2+}, and Zn^{2+}, which enables the potential application of detection of Hg^{2+} in water samples by naked eyes. The absorbance ratio A_{440}/A_{380} linearly increased by increasing the Hg^{2+} concentration from 4.5 to 16.5 μmol·L^{-1} (Fig. 1b, Inset). The two isosbestic points at 308 and 403 nm reveal the existence of only one intermediate complex (Fig. 1b). The Job's plot obtained by varying the concentration ratio of Hg^{2+} and **1** gained the 1∶1 combined stoichiometric ratio of **1** and Hg^{2+} (Fig. S3), with an association constant (K_a) of 3.48×10^4 L·mol^{-1} according to the Benesi-Hildebrand expression (Fig. S4)[21]. The limit of detection (LOD) of **1** to Hg^{2+} was 59.6 nmol·L^{-1} based on $3\sigma/k$ (σ: standard deviation, k: slope)[20], which was lower than the LOD of **1a**.

2.3 Fluorescence spectroscopic studies for Hg^{2+} sensor activity

Fluorescence emission spectral changes of **1**, caused by the presence of several metal ions in the EtOH/H_2O (7∶3, *V*/*V*) solution, are demonstrated in Fig.2. When excited at 410 nm, the initial solution of **1** displayed a weak emission at 475 nm (quantum yield Φ =0.02, determined with quinine sulfate, and Φ_c= 0.546 in 0.05 mol·L^{-1} H_2SO_4)[22]. Significant changes in the emission spectrum were observed in the presence of Hg^{2+} (3 equiv.), except in the case of other metal cations (3 equiv.). When **1** was combined with Hg^{2+} (3 equiv.), the fluorescence intensity was significantly enhanced as the color changed from colorless to cyan (Fig. 2a, Inset) under a 365 nm UV lamp (Φ =0.21). Furthermore, it can be seen from Fig.S5 that the average decay constant (τ) value of **1** obtained by the single exponential decay fitting method was 1.56 ns, which was far less than that of **1**-Hg^{2+} (6.12 ns), indicating the coordination between **1** and Hg^{2+}.

Similarly, the linear response concentration range of Hg^{2+} was 6.0-18.0 μmol·L^{-1} according to the fluorescent titration results (Fig. 2b, Inset). The K_a and LOD were 2.61×10^4 L·mol^{-1} (Fig. S6) and 45.8 nmol·L^{-1}, respectively, which are in the same order of magnitude when compared with the data from UV spectra. All these facts show that the response of probe **1** to Hg^{2+} is characterized by efficient selectivity and sensitivity in colorimetric and fluorescent detection, so it can be used to research Hg^{2+} quantitatively in water or biological samples.

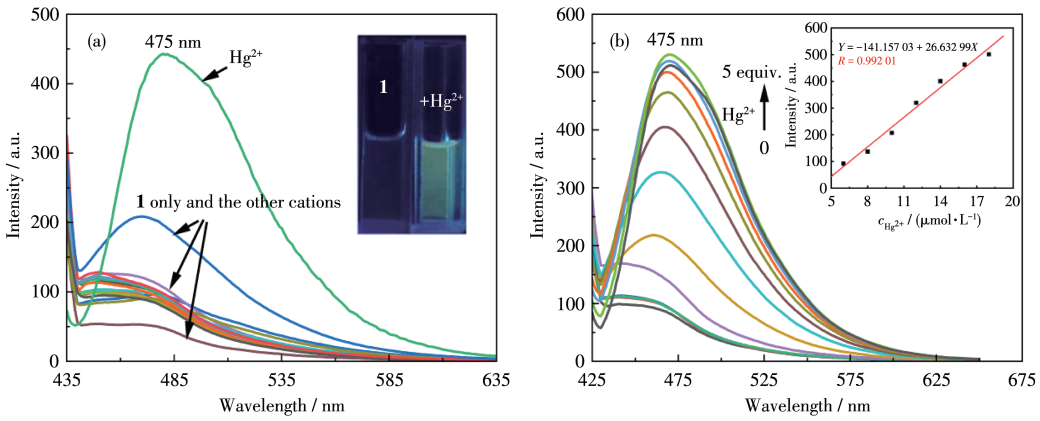

Inset in a: the color change of **1** solution in the presence of Hg^{2+} under 365 nm UV lamp; Inset in b: the fluorescence intensity at 475 nm as a function of Hg^{2+} concentration (6.0-18.0 μ mol·L^{-1}); λ_{ex}=410 nm

Fig.2 (a) Fluorescence emission spectra of 10 μmol·L^{-1} probe **1** in EtOH/H_2O (7∶3, *V*/*V*) solution with 3 equiv. of metal ions: Ag^+, Al^{3+}, Ca^{2+}, Cd^{2+}, Co^{2+}, Cr^{3+}, Cu^{2+}, Fe^{3+}, Hg^{2+}, K^+, Mg^{2+}, Mn^{2+}, Na^+, Ni^{2+}, Pb^{2+}, and Zn^{2+} ions and blank. The inset shows. (b) Fluorescence emission spectra of 10 μmol·L^{-1} probe **1** upon the addition of Hg^{2+} (0-5 equiv.) in EtOH/H_2O (7∶3, *V*/*V*) solution

2.4 Investigation of environmental factors and dynamics analysis

The specificity of Hg^{2+} to probe **1** was determined by testing the interference of other metal cations (Fig. S7 and S8). No distinct changes in the UV and fluorescence spectra of **1**+Hg^{2+} were observed in the presence of other metal cations, in addition to trivalent cations (Al^{3+}, Cr^{3+}, and Fe^{3+}) in which their strong Lewis acidity results in imine-bond cleavage[23], thereby indicating that the ability of probe **1** to detect Hg^{2+} is less affected by other metal cations and has high selectivity.

It was concluded that **1** can detect Hg^{2+} in a pH range of 4.0 to 10.0 by studying the fluorescence intensity changes of probe **1** and probe **1**+Hg^{2+} at different pH values (Fig.S9). Due to this unique property, probe **1** can be used for practical studies of Hg^{2+} in lysosomes. Compared with the probe **1a** described in our previous work[14], the introduction of 4-(2-aminoethyl) morpholine not only improves the selectivity of the probe (interference from Cu^{2+} in the case of **1a**) but also enhances the tolerance to acidic environments.

A fast time response is an important characteristic of chemosensors. The changes in the fluorescence of **1** (10 mol·L^{-1}) in EtOH/H_2O (7∶3, *V*/*V*) solution with 3 equiv. of Hg^{2+} was detected in less than 2 min, which is a faster analysis time for the Hg^{2+} detection than that of **1a** (*ca*. 3 min) (Fig.S10).

The reversibility of the probe toward Hg^{2+} was investigated by adding EDTA to the **1**+Hg^{2+} system. The results showed that the emission of **1**+Hg^{2+} was totally quenched upon the addition of EDTA (3 equiv.), and it was recovered by further addition of Hg^{2+}. The on-off phenomenon was reversible even after four cycles (Fig.S11), indicating that the probe can be easily regenerated for repeated use.

2.5 Reaction mechanism

To analyze the coordination mechanism of **1** with Hg^{2+}, ESI-MS measurements were performed in EtOH solution (Fig. 3). The spectrum of **1**+Hg^{2+} displayed a peak at *m*/*z* 754.275 1 corresponding to the protonated cation of [Hg(**1**−2H)] (**1**-Hg^{2+}, $C_{28}H_{40}N_8O_4Hg$, Calcd. 753.29). Furthermore, in the ^{1}H NMR spectrum of **1**+Hg^{2+} (Fig.4), the signal of the CH═N groups of **1** at δ 8.40 shifted to the lower field and split into two peaks at δ 8.50 and 8.60, indicating the coordination of one imine N atom and the change in the environment of the other imine N atom. The amide NH signal of **1** was greatly broadened at δ 7.24 and significantly shifted to δ 7.89 in the presence of Hg^{2+}, it may be because of the effect of the two pyrrole N atoms to protons and coordination effect. Therefore, a donor set of two pyrrole and one imine N atoms involving the binding of Hg^{2+} is suggested, as illustrated in Scheme 2.

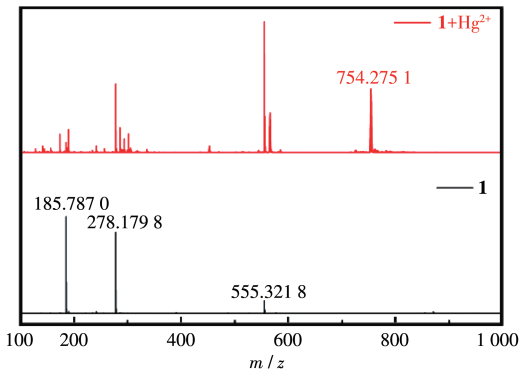

Fig.3 ESI-MS spectral changes of **1** with the addition of Hg^{2+} in EtOH solution

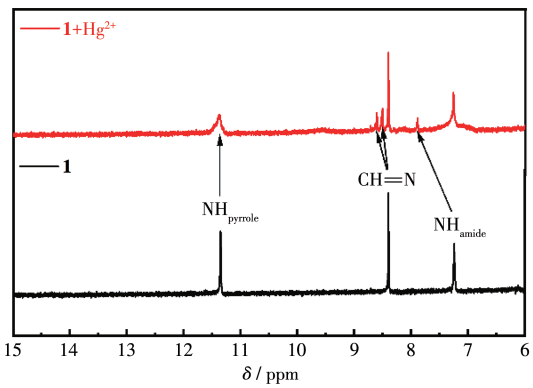

Fig.4 ^{1}H NMR spectral changes of **1** with the addition of Hg^{2+} in DMSO-d_6 solution

To gain more insights into the sensing mechanism, **1** and **1**-Hg^{2+} were examined by density functional theory (DFT) calculation[24]. The results show that both HOMO and LUMO are dispersed on pyrrole and imine moieties in probe **1** (Fig. 5), while the C═N isomerization leads to weak fluorescence. In contrast, the C═N isomerization is not possible in the **1**-Hg^{2+} complex. Meanwhile, the HOMO of **1**-Hg^{2+} is localized on the pyrrole and imine moieties, while the LUMO is

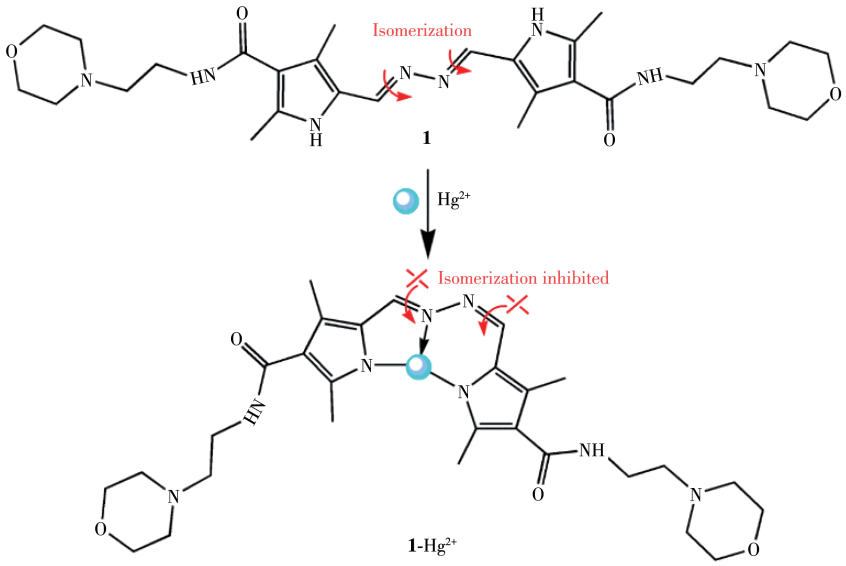

Scheme 2　Proposed reaction mechanism of **1** with Hg^{2+} ions

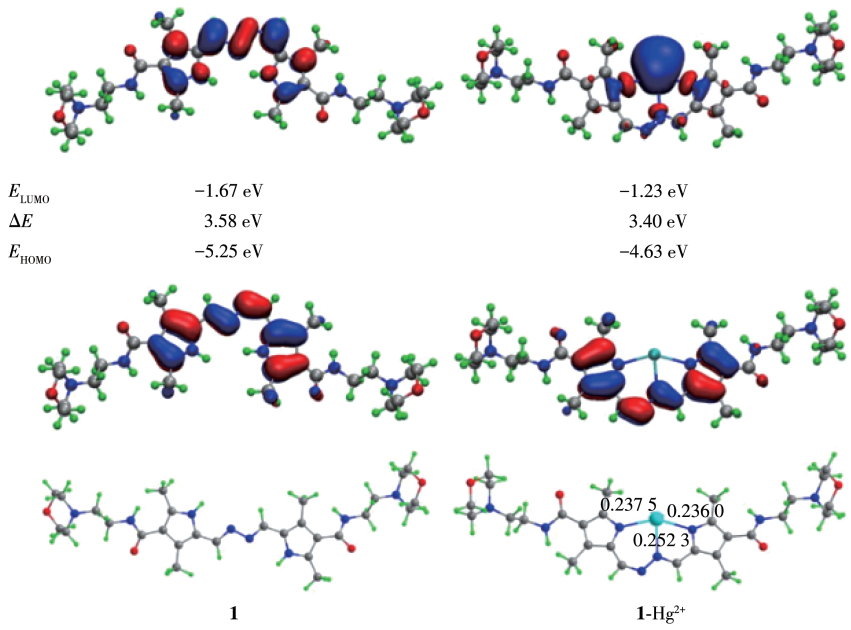

Fig.5　Optimized structures and HOMO/LUMO of **1** and **1**-Hg^{2+} by DFT calculation

almost centered on the Hg^{2+} ion, clearly indicating that the emission of **1**-Hg^{2+} is mainly from the LMCT. The corresponding energy difference (ΔE) of **1**-Hg^{2+} (3.40 eV) is lower than that of **1** (3.58 eV), reflecting the longer maximum absorbance wavelength of **1**-Hg^{2+} compared to that of **1**. The Hg—$N_{pyrrole}$ bond lengths in complex **1**-Hg^{2+} were 0.236 0 and 0.237 5 nm, respectively, which are shorter than that of Hg—N_{imine} (0.253 2 nm). Nevertheless, these bond lengths are comparable with those in the calculated **1a**-Hg^{2+} complex, thus suggesting stable emission of complex **1**-Hg^{2+} in an aqueous solution[14].

2.6　Bioimaging applications

The MTT assay was used to detect the effect of probe **1** on cell viability as shown in Fig.S12, the cell viability was still 82.6% even while the probe concentration reached 40 $\mu mol \cdot L^{-1}$, which indicates that probe **1** had low cytotoxicity. The biological suitability of probe **1** was assessed by detecting its ability to examine Hg^{2+} in HeLa cells. HeLa cells without the treatment of probe **1** exhibited no fluorescence signal (Fig.6a), while after incubation with **1** (10 $\mu mol \cdot L^{-1}$) at

37 ℃ for 30 min, a faint blue fluorescence was observed in the cells (Fig.6d), which should be attributed to the emission of probe **1**. Next, the brighter cellular blue fluorescence was shown after the cells were treated with 20 μmol·L^{-1} Hg^{2+} (Fig.6g). This finding indicates the capability of **1** in imaging Hg^{2+} in living cells.

To determine the capability of **1** to detect Hg^{2+} in the lysosomes of HeLa cells, colocalization images were performed with LysoTracker Red (Fig.7). When the image was merged, it could be observed that the

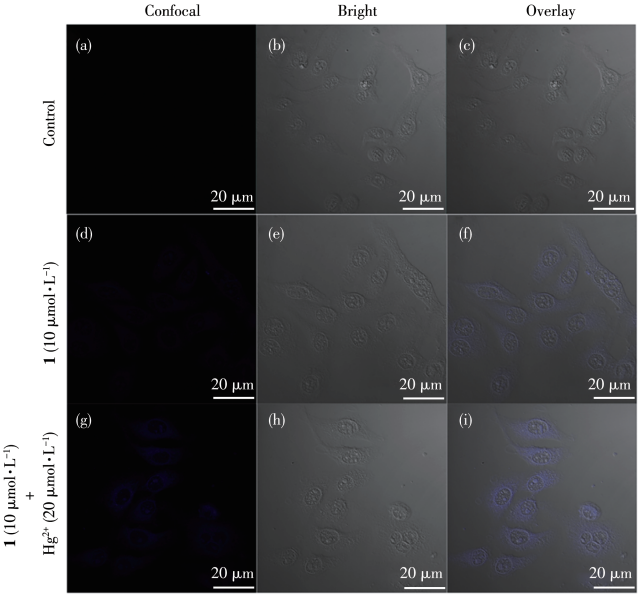

Fig.6 Confocal fluorescence images of Hela cells: confocal fluorescence (a), brightfield (b), and overlay (c) images of HeLa cells incubated for 30 min at 37 ℃; confocal fluorescence (d), brightfield (e), and overlay (f) images of HeLa cells incubated with 10 μmol·L^{-1} of 1 for 30 min at 37 ℃; confocal fluorescence (g), brightfield (h), and overlay (i) images of HeLa cells incubated with 10 μmol·L^{-1} of **1** for 30 min at 37 ℃ and then incubated with 20 μmol·L^{-1} Hg^{2+} for another 30 min at 37 ℃

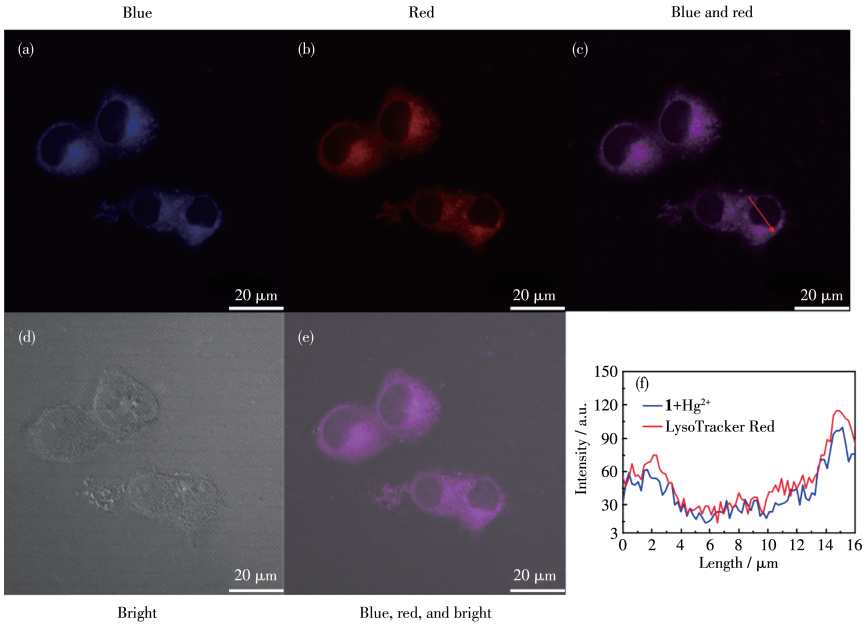

Fig.7 Bright field and fluorescence images of HeLa cells stained with 10 μmol·L^{-1} of probe **1**+Hg^{2+} (20 μmol·L^{-1}) and LysoTracker Red: (a) from the blue channel, (b) from the red channel (lysosomes staining), (c) an overlay blue and red channels, (d) bright field image, (e) an overlay of bright field, blue, and red channels; (f) Intensity profile of the linear region of interest across the HeLa cell co-stained with LysoTracker Red and the blue channel of **1**+Hg^{2+}

blue fluorescence channel of **1**+Hg^{2+} has a coincidence rate of 0.91 with the red channel of the lysosome tracker. The above results indicate that the probe can detect Hg^{2+} in the lysosomes of living cells.

3 Conclusions

In summary, a pyrrole-based bis-hydrazone appended with 4-(2-aminoethyl)morpholine moiety has been prepared, which acts as a fluorescent off-on sensor toward Hg^{2+}. The mechanism was completely investigated by UV-Vis, fluorescence spectroscopy, time-resolved fluorescence spectroscopy, ESI-MS, ^{1}H NMR, and DFT calculations. Probe **1** can be used as an Hg^{2+} sensor. In addition, the costained experiment reveals that the probe was able to image Hg^{2+} in lysosomes.

Supporting information is available at http://www.wjhxxb.cn

References:

[1]成昭, 梁静, 任熙玲, 崔誉文, 杨莉宁. 有机小分子Zn^{2+}荧光探针与生命体中Zn^{2+}示踪的研究进展. 化学世界, **2021**,**62**(12):707-716
CHENG Z, LIANG J, REN X L, CUI Y W, YANG L N. Research progress in organic small-molecule fluorescent Zn^{2+} probes and fluorescent imaging analysis of biological Zn^{2+}. *Chemical World*, **2021**,**62**(12):707-716

[2]Marumoto M, Sakamoto M, Marumoto K, Tsuruta S, Komohara Y. Mercury and selenium localization in the cerebrum, cerebellum, liver, and kidney of a Minamata disease case. *Acta Histochem. Cytochem.*, **2020**, **53**(6):147-155

[3]Kim K H, Kabir E, Jahan S A. A review on the distribution of Hg in the environment and its human health impacts. *J. Hazard. Mater.*, **2016**,**306**:376-385

[4]Erdemir S, Kocyigit O, Malkondu S. Detection of Hg^{2+} ion in aqueous media by new fluorometric and colorimetric sensor based on triazole-rhodamine. *J. Photochem. Photobiol. A*, **2015**,**309**:15-21

[5]Sarkar A, Chakraborty S, Lohar S, Ahmmed E, Saha N C, Mandal S K, Dhara K, Chattopadhyay P. A lysosome-targetable fluorescence sensor for ultrasensitive detection of Hg^{2+} in living cells and real samples. *Chem. Res. Toxicol.*, **2019**,**32**(6):1144-1150

[6]Yuan X, Leng T H, Guo Z Q, Wang C Y, Li J Z, Yang W W, Zhu W H. A FRET-based dual-channel turn-on fluorescence probe for the detection of Hg^{2+} in living cells. *Dyes Pigm.*, **2018**,**161**:403-410

[7]Wang Y S, Ding H C, Wang S, Fan C B, Tu Y Y, Liu G, Pu S Z. A ratiometric and colorimetric probe for detecting Hg^{2+} based on naphthalimide rhodamine and its staining function in cell imaging. *RSC Adv.*, **2019**,**9**(21):11664-11669

[8]Lan L X, Niu Q F, Li T D. A highly selective colorimetric and ratiometric fluorescent probe for instantaneous sensing of Hg^{2+} in water, soil and seafood and its application on test strips. *Anal. Chim. Acta*, **2018**,**1023**:105-114

[9]侯淑华, 李仕琦, 汤立军. 新型水溶性罗丹明类荧光探针的合成及其对游离3价金属离子的识别. 应用化学, **2022**,**39**(2):241-246
HOU S H, LI S Q, TANG L J. Synthesis of a novel water-soluble rhodamine-based fluorescent probe and its selective detection of free trivalent ions. *Chinese Journal of Applied Chemistry*, **2022**,**39**(2):241-246

[10]Wu C J, Wang J B, Shen J J, Bi C, Zhou H W. Coumarin-based Hg^{2+} fluorescent probe: Synthesis and turn-on fluorescence detection in neat aqueous solution. *Sens. Actuator B-Chem.*, **2017**,**243**:678-683

[11]Zhang Y F, Chen H Y, Chen D, Wu D, Chen Z, Zhang J, Chen X Q, Liu S H, Yin J. A colorimetric and ratiometric fluorescent probe for mercury(Ⅱ) in lysosome. *Sens. Actuator B-Chem..*, **2016**,**224**:907-914

[12]孙京府, 钱鹰. 一种萘酰亚胺-罗丹明衍生物的合成、聚集诱导荧光增强及其双通道荧光探针性能. 有机化学, **2016**,**36**(1):151-157
SUN J F, QIAN Y. A novel naphthalimide-rhodamine fluorescence sensor: synthesis, aggregation-induced emission enhancement and its dual-channel detection property. *Chin. J. Org. Chem.*, **2016**,**36**(1):151-157

[13]Vinoth Kumar G G, Kesavan M P, Tamilselvi A, Rajagopal G, Raja J D, Sakthipandi K, Rajesh J, Sivaraman G. A reversible fluorescent chemosensor for the rapid detection of Hg^{2+} in an aqueous solution: Its logic gates behavior. *Sens. Actuator B-Chem.*, **2018**,**273**:305-315

[14]Wang Y, Mao P D, Wu W N, Mao X J, Fan Y C, Zhao X L, Xu Z Q, Xu Z H. New pyrrole-based single-molecule multianalyte sensor for Cu^{2+}, Zn^{2+}, and Hg^{2+} and its AIE Activity. *Sens. Actuator B-Chem.*, **2018**,**255**:3085-3092

[15]Zhu J L, Xu Z, Yang Y, Xu L. Small-molecule fluorescent probes for specific detection and imaging of chemical species inside lysosomes. *Chem. Commun.*, **2019**,**55**(47):6629-6671

[16]Yuan L L, Shi X J, Tang B Z, Wang W X. Real-time *in vitro* monitoring of the subcellular toxicity of inorganic Hg and methylmercury in zebrafish cells. *Aquat. Toxicol.*, **2021**,**236**:105859

[17]Lauwerys R, Buchet J P. Study on the mechanism of lysosome labilization by inorganic mercury *in vitro*. *Eur. J. Biochem.*, **1972**,**26**(4):535-542

[18]He D D, Liu W, Sun R, Fan C, Xu Y J, Ge J F. *N*-pyridineium-2-yl Darrow Red analogue: Unique near-infrared lysosome-biomarker for the detection of cancer cells. *Anal. Chem.*, **2015**,**87**(3):1499-1502

[19]普特, 杨云海, 王凯博, 叶敏, 范黎明, 付立新, 苏发武, 查友贵. MTT比色法测定烟酰胺类化合物对植物病原细菌的抑菌活性. 云南农业大学学报(自然科学), **2019**,**34**(1):15-21
PU T, YANG Y H, WANG K B, YE M, FAN L M, FU L X, SU F W, ZHA Y G. Determination of the nicotinamide compounds by using MTT colorimetric assay against pathogenic bacteria. *J. Yunnan Agric. Univ.* (*Natural Science*), **2019**,**34**(1):15-21

[20]Wu W N, Wu H, Zhong R B, Wang Y, Xu Z H, Zhao X L, Xu Z Q, Fan Y C. Ratiometric fluorescent probe based on pyrrole-modified rhodamine 6G hydrazone for the imaging of Cu^{2+} in lysosomes. *Spectroc. Acta Pt. A-Molec. Biomolec. Spectr.*, **2018**,**212**:121-127

[21]Wang Y, Chang H Q, Wu W N, Zhao X L, Yang Y, Xu Z Q, Xu Z H, Jia L. Rhodamine-2-thioxoquinazolin-4-one conjugate: A highly sensitive and selective chemosensor for Fe^{3+} ions and crystal structures of its Ag(Ⅰ) and Hg(Ⅱ) complexes. *Sens. Actuator B-Chem.*, **2017**,**239**: 60-68

[22]Wu W N, Mao P D, Wang Y, Zhao X L, Xu Z Q, Xu Z H, Xue Y. Quinoline containing acetyl hydrazone: An easily accessible switch-on optical chemosensor for Zn^{2+}. *Spectroc. Acta Pt. A-Molec. Biomolec. Spectr.*, **2018**,**188**:324-331

[23]Qin J C, Fan L, Yang Z Y. A small-molecule and resumable two-photon fluorescent probe for Zn^{2+} based on a coumarin Schiff-base. *Sens. Actuator B-Chem.*, **2016**,**228**:156-161

[24]Jia F Y, Luo J W, Zhang B. Mechanistic insight into palladium-catalyzed enantioselective remote meta-C-H arylation and alkylation by using density functional theory (DFT) calculations. *Adv. Synth. Catal.*, **2020**,**362**(8):1686-1695